blood

Prepublished online Sep 29, 2009;
doi:10.1182/blood-2009-05-219634

In vivo intra- and inter-clonal kinetic heterogeneity in B-cell chronic lymphocytic leukemia

Carlo Calissano, Rajendra N. Damle, Gregory Hayes, Elizabeth J. Murphy, Marc K. Hellerstein, Carol Moreno, Cristina Sison, Matthew S. Kaufman, Jonathan E. Kolitz, Steven L. Allen, Kanti R. Rai and Nicholas Chiorazzi

Blood (print ISSN 0006-4971, online ISSN 1528-0020), is published semimonthly by the American Society of Hematology, 1900 M St, NW, Suite 200, Washington DC 20036.

In vivo intra- and inter-clonal kinetic heterogeneity in B-cell chronic lymphocytic leukemia

Running title: *In vivo* kinetic heterogeneity in CLL

By

Carlo Calissano[1], Rajendra N. Damle[1,2], Gregory Hayes[3], Elizabeth J. Murphy[3,4], Marc K. Hellerstein[3], Carol Moreno[1], Cristina Sison[5], Matthew S. Kaufman[6], Jonathan E. Kolitz[1,2], Steven L. Allen[1,7], Kanti R. Rai[1,6], and Nicholas Chiorazzi[1,6,8]

[1] The Feinstein Institute for Medical Research, North Shore - LIJ Health System, Manhasset, NY

[2] Departments of Medicine, North Shore University Hospital, North Shore – LIJ Health System, Manhasset, NY, and NYU School of Medicine, NY, NY

[3] KineMed, Inc., 5980 Horton Street, Emeryville, CA

[4] Department of Medicine, University of California, San Francisco

[5] Biostatistics Unit, The Feinstein Institute for Medical Research, North Shore - LIJ Health System, Manhasset, NY

[6] Departments of Medicine, Long Island Jewish Medical Center, North Shore – LIJ Health System, New Hyde Park, NY, and Albert Einstein College of Medicine, Bronx, NY

[7] Departments of Medicine, North Shore University Hospital, North Shore – LIJ Health System, Manhasset, NY, and Albert Einstein College of Medicine, Bronx, NY

[8] Department of Cell Biology, Albert Einstein College of Medicine, Bronx, NY

Address correspondence to:

Nicholas Chiorazzi, M.D.
The Feinstein Institute for Medical Research
350 Community Drive
Manhasset, NY 11030
Phone: 516-562-1090
Fax: 516-562-1011
Email: NChizzi@NSHS.edu

Abstract

Clonal evolution and outgrowth of cellular variants with additional chromosomal abnormalities are major causes of disease progression in chronic lymphocytic leukemia (CLL). Because new DNA lesions occur during S phase, proliferating cells are at the core of this problem. In this study, we used *in vivo* ^{2}H-labeling of CLL cells to better understand the phenotype of proliferating cells in 13 leukemic clones. In each case, there was heterogeneity in cellular proliferation, with a higher fraction of newly-produced $CD38^{+}$ cells compared to $CD38^{-}$ counterparts. On average, there were two fold higher percentages of newly-born cells in the $CD38^{+}$ fraction than in $CD38^{-}$ cells; when analyzed on an individual patient basis, $CD38^{+}$ ^{2}H-labeled cells ranged from 6.6 to 73%. Based on distinct kinetic patterns, inter-clonal heterogeneity was also observed. Specifically, four patients exhibited a delayed appearance of newly-produced $CD38^{+}$ cells in the blood, higher leukemic cell CXCR4 levels, and increased risk for lymphoid organ infiltration and poor outcome. Our data refine the proliferative compartment in CLL based on CD38 expression and suggest a relationship between *in vivo* kinetics, expression of a protein involved in CLL cell retention and trafficking to solid tissues, and clinical outcome.

Introduction

B-cell chronic lymphocytic leukemia (CLL) is a relatively common and incurable adult disease of unknown etiology. Although the vast majority of circulating CLL cells are not proliferating[1,2], a small proliferative compartment does exist[3], and lymph nodes and bone marrow contain aggregates of activated, dividing cells[4]. In addition, accessory signals delivered in the microenvironment of these solid tissues are essential for neoplastic cell survival and expansion[5], suggesting that clonal accumulation involves rescue of leukemic cells from death. Thus, a dynamic balance between birth and death is characteristic of CLL clones[3].

The disease has a strikingly variable clinical course, and different biological variables help predict clinical outcome[6,7], including Ig heavy variable (*IGHV*) gene mutation status[8] and the percent of cells expressing ZAP-70[9,10] and CD38[6,11]. CD38 is a surface membrane bound ecto-enzyme that functions as a receptor[12-15]. Expression of CD38 on normal B cells depends on cell maturation and can be induced upon stimulation[16]. The prognostic value of CD38 is linked to its capacity to promote leukemic cell survival[17-20]. Moreover, within each CLL clone, cells expressing CD38 are enriched in expression of Ki-67[21], suggesting that $CD38^+$ cells represent a cycling subset.

Deuterium (^2H) incorporation into newly-synthesized DNA can be precisely quantified by Gas Chromatography/Mass Spectrometry (GC/MS) providing an established measure of DNA replication[22,23]. This approach documented that *in vivo* CLL cells proliferate at rates ranging from 0.08% - 1.7% of the clone per day[3,24], and patients with higher birth rates appear at risk of more active disease[3].

In this study, we used *in vivo* ^2H-labeling to better understand the phenotype of the most actively proliferating cells within each CLL clone. ^2H-enrichment in genomic DNA was

compared between $CD38^+$ and $CD38^-$ cells of 13 patients, revealing intra-clonal heterogeneity in cellular proliferation, with $CD38^+$ cells proliferating more rapidly. We also identified inter-clonal heterogeneity with two patient groups of distinct kinetic patterns and CXCR4 levels. The group with higher CXCR4 levels showed a delayed appearance of ^2H-labeled $CD38^+$ cells in blood and seemed at a higher risk for lymphoid organ infiltration and inferior outcome. Our data suggest relationships between CLL kinetics, expression of a molecule involved in CLL cell retention and trafficking to solid tissues[25,26], and clinical course.

Material and Methods

Patients and ^2H_2O protocols. The study was approved by the North Shore - LIJ Health System's Institutional Review Board and was conducted according to the principles of the World Medical Association Declaration of Helsinki. Thirteen CLL patients (Table 1), diagnosed by established criteria[27], were selected from a larger cohort who participated in ^2H_2O protocols. All subjects provided written informed consent prior to enrollment. Exclusion criteria for patient participation can be found in Supplemental Materials and Methods. Every patient received ^2H, in the form of ^2H_2O, during a labeling period (6 to 12 weeks) and was followed until the end of washout period (week 24) in accordance to protocols reported in Supplemental Material and Methods. CLL cells were studied at three time points (Figure 1A). Because previously published data showed delayed appearance of labeled cells in the blood of some patients[3], time points were selected (a) during the labeling period (3 or 4 weeks), (b) at or near the end of the labeling period (6 or 8 weeks), and (c) after ^2H_2O washout (usually week 24).

Isolation of cell fractions based on expression of CD38 and Ki-67.

CD38: Previously cryopreserved PBMCs from CLL patients were thawed and incubated with murine monoclonal IgG1 anti-human CD5-FITC, CD38-PE, CD3-PerCP and CD19-APC (all from BD Biosciences, San Jose, CA). After sorting into $CD19^+CD5^+CD38^+$ and $CD19^+CD5^+CD38^-$ fractions with a BD FACSAria™ (Becton Dickinson Immunocytometry systems, San Jose, CA) (Figure 1B), cells were washed, pelleted, and stored at -80° until performing GC/MS.

Ki-67: Cells from CLL452 and CLL625 were labeled with anti-CD38-PE, -CD3-PerCP, -CD19-APC and -CD5-PECy7 (all BD Biosciences), permeabilized and fixed (Cytofix/Cytoperm

solution; BD Biosciences), and then stained intracellularly with murine mAb to Ki-67-FITC (BD Biosciences). Fractions were sorted and stored as above.

Determination of Ki-67, ZAP-70 and chemokine receptor levels. Ki-67 expression was determined by flow cytometry after labeling cells with the panel of mAbs mentioned above. For ZAP-70, cells were incubated with murine monoclonal IgG1 anti-human CD5-PE, CD3-PerCP and CD19-APC (BD Biosciences), permeabilized and fixed (Cytofix/Cytoperm solution; BD Biosciences), and then stained intracellularly with mAb to ZAP-70-FITC (eBiosciences, San Diego, CA). For chemokine receptors, the following murine mAbs were used: CD38-APC, CD19-PerCP, CD5-FITC (BD Biosciences) as well as, CCR1, CCR2, CCR7, CXCR1, CXCR4 [clone 12G5] and CXCR5 (R&D Systems, Minneapolis, MN), CCR4, CCR5, CXCR2, CXCR3 (BD Biosciences); all anti-chemokine receptor mAbs were conjugated to phycoerythrin (PE). All data were acquired with a BD LSRII flow cytometer (Becton Dickinson Immunocytometry systems) and analyzed by FlowJo v7.2.4 version.

Culture conditions to analyze ^{2}H dilution in proliferating cells. PBMCs from CLL355, taken when the highest ^{2}H-enrichment was found (Table 2), were labeled with carboxyfluorescein succinimidyl ester (CFSE; Molecular Probes/Invitrogen, Carlsbad, CA) at a final concentration of 10μM/10^{7} cells. An aliquot of cells was analyzed as a measure of CFSE intensity on day 0, and the remaining cells cultured for five days ($4x10^{6}$/ml) over a layer of irradiated CD32-transfected murine fibroblasts (ATCC, Manassas, VA) at a fibroblast/PBMC ratio of 1/10. Interleukin (IL)-15, IL-2 (both 5ng/ml; R&D Systems) and CpG 2006-G5 (0.5μg/ml; InvivoGen, San Diego, CA) were added. When harvested, the absolute number of cells was determined with

Countbright™ beads for flow cytometry (Invitrogen) according to instructions. B cells were identified using CD19-APCcy7 (BD Biosciences) and sorted on a BD FACSAria™ based on CFSE labeling.

Measurement of body ^2H_2O-enrichment. Total body water ^2H_2O enrichment was determined by MS[28] at multiple time points from serum or plasma (Figure 1A).

Measurement of ^2H-enrichment in deoxy-adenosine of DNA. Deuterium incorporated from ^2H_2O into the deoxyribose moiety of adenosine (dA), was quantified by GC/MS as the molar excess fraction (EM_1) above natural occurrence by subtraction of an unlabeled DNA standard from calf thymus as described[22,23]. See also Supplemental Materials and Methods.

Calculation of fraction (f) of new cells. The fraction (%) of labeled new cells, *f*, was calculated from EM_1 and the precursor enrichment (p), which was the average body water % ^2H_2O at plateau. The asymptotic or maximal EM1* was calculated using the following equation: EM1* = $-7.7268p^2 + 3.5291p + 0.0023$,[22]. *f* was then calculated as *f* = EM1/EM1*.

Analysis of IGHV mutations in CLL cells. *IGHV* mutation status was determined as described[8].

Quantification of mean telomere lengths. A flow cytometry-fluorescence in situ hybridization (Flow-FISH) protocol was used as published[29].

Cytogenetic analysis. Cytogenetic analyses were performed by FISH using the following probes: chromosome 11, LSI ATM at 11q22.3; chromosome 12, CEP-12 centromere; chromosome 13, LSI D13S319 at 13q14.3 and LSI 13q34 at 13q34; and chromosome 17, LSI p53 at 17p13.1 (all from Vysis, Inc., Downers Grove Il).

Statistical analyses. A mixed model repeated measures analysis was used to determine if the ratio of the percent labeled $CD38^+$ to percent labeled $CD38^-$ cells (expressed as log of the ratio) differed across the 3 time points and whether the patterns of change over time of this ratio were significantly different across the 3 protocol groups (Figure 1). All pairwise comparisons were carried out using a Bonferroni adjustment. For data in Table 2, a paired t-test was used within each time point. Classification of patients into Group A and Group B (Figure 3) was based on slopes of the lines generated by the percent labeled cells in $CD38^+$ and $CD38^-$ fractions from time points 2 to 3, and declaring slopes as concordant positive (CP), if both $CD38^+$ and $CD38^-$ lines exhibited positive slopes, or non-CP, otherwise. Fisher's Exact test was used to compare clinical data between Group A and Group B patients. White blood cell (WBC) counts were compared using a mixed model repeated measures analysis. The Mann-Whitney test was used for data in Figure 5.

Results

Intra-clonal heterogeneity: $CD19^+CD5^+CD38^+$ cells proliferate more rapidly than $CD19^+CD5^+CD38^-$ cells. In this study we asked if all cells in a CLL clone divide at the same rate and, if not, how to identify those subpopulations that divide more rapidly. Given the known biologic and clinical value of CD38[6,15], we measured ^2H-incorporation into $CD38^+$ and $CD38^-$ fractions of leukemic clones from 13 patients who participated in ^2H_2O-labeling studies. ^2H-enrichment was measured in genomic DNA from $CD19^+CD5^+CD38^+$ and $CD19^+CD5^+CD38^-$ cells at three time points (Figure 1A-B), and these values were used to calculate *f*, percent newly-produced CLL cells.

We found (Table 2) a two-fold higher percentage of newly-produced cells in the $CD38^+$ compared to the $CD38^-$ compartment at both time points during labeling period (16.5% ± 3.9 vs. 7.3% ± 1.8 at 1st time point, $P < 0.01$; 25.9% ± 5.4 vs. 11.2% ± 1.7 at 2nd time point, $P = 0.013$). When analyzed on an individual patient basis, a larger *f* was found in the $CD38^+$ population of all but one patient (CLL280 at only the 1st time point), with maximum numbers ranging from 6.6% to 73% (CLL 875 and 606, respectively).

When presented as a ratio of all patients (Figure 1C), newly-labeled cells (*f*) in the $CD38^+$ fractions are ~2.5 times greater than in the $CD38^+$ fraction at both time points. Of note, observed differences did not correlate with the number of $CD38^+$ cells in individual CLL clones prior to fractionation (range 1% - 98%; Table 1). For example, when analyzing data from cells taken at the 1st time point, $CD38^+$ to $CD38^-$ labeled fraction ratios were >2 in 6 patients (CLL 452, 546, 569, 606, 822, 931; Table 2) and the percent of $CD38^+$ cells in these clones ranged from 7% to 98% (Table 1).

Within each CLL clone, the Ki-67$^+$ fraction is enriched in CD38$^+$ cells and has more ^{2}H incorporated in genomic DNA. Ki-67 is a cell cycle related molecule[30], and Ki-67-expressing cells are enriched in CD38$^+$ fractions of individual CLL clones[21]. As illustrated by CLL822, the Ki-67$^+$ fraction (5.5%; upper right) was markedly enriched in CD38$^+$ cells (83%; Figure 2A, lower right). Similar enrichments of CD38$^+$ cells in Ki-67$^+$ fractions were found in all patients tested (Supplemental Figure 1).

To directly prove that Ki-67 expression represents proliferating cells in CLL, CD19$^+$CD5$^+$ cells from CLL452 obtained at the three time points were sorted into four fractions based on expression of Ki-67 and CD38 (Figure 2B). Consistent with phenotypic data[31], *f* was higher among cells expressing Ki-67 at both time points during the labeling period, with a hierarchy of incorporation: CD38$^+$Ki-67$^+$ > CD38$^-$Ki-67$^+$ > CD38$^+$Ki-67$^-$ > CD38$^-$Ki-67$^-$. Of note, the CD38$^+$Ki-67$^+$ fraction contained ~50% newly divided cells and the Ki-67$^+$ cells represented a highly proliferating subset, defined by ^{2}H-incorporation in DNA, regardless of the expression of CD38. Similar findings were obtained from CLL625 (Figure 2C). In this case, 70% of cells in the CD38$^+$Ki-67$^+$ fraction were new and already at plateau by 21 days of labeling, suggesting a minimum estimated cellular turnover rate of 3.3% per day (70%/21 days), ~2 – 30 fold higher than the rates previously observed for whole CLL clones[3,24].

Differences in proliferative rates between CD19$^+$CD5$^+$CD38$^+$ and CD19$^+$CD5$^+$CD38$^-$ cells are no longer evident after ^2H_2O washout. The rate at which the fraction of ^{2}H-labeled cells of a population with a high turnover (e.g., PMNLs) disappears from blood after ^2H_2O intake cessation (washout period) is relatively rapid and follows the decline of available ^2H_2O[4]. In this study, at the end of the washout period we observed a diminution in the fraction of ^{2}H-containing

$CD38^+$ cells, accompanied by stability or increase in the $CD38^-$, ^2H-labeled fraction in many cases (Table 2). As a result, *f* was no longer different ($CD38^+$ vs. $CD38^-$; 15.2% ± 2 vs. 13.7% ± 2.1; $P = 0.25$) and the ratio of *f* of the two fractions was essentially one. Mean ratios recorded during labeling periods (time point 1 and 2) were significantly different from those recorded at time point 3 (Figure 1C). A decrease in the ratios of $CD38^+$ to $CD38^-$ newly-produced cells between 2nd and 3rd time point was observed in 11 of 13 patients (Table 2).

Telomere length measurements of $CD38^+$ and $CD38^-$ fractions. The ^2H-incorporation data presented above indicate that within each CLL clone, $CD38^+$ cells divide faster than $CD38^-$. We wanted to determine if the differences in newly-produced cells were reflected by differences in telomere lengths.

Notably, an average of the mean telomere lengths of the 13 CLL clones and their CD38-defined fractions did not correspond with proliferation data obtained by ^2H-incorporation (Table 3). $CD38^+$ subsets had shorter telomere lengths compared to $CD38^-$ ones in only 5/13 patients. Moreover, some patients in whom higher ^2H fractional enrichments in $CD38^+$ cells were most evident (CLL 546 and 569) had longer telomere lengths, compared to $CD38^-$ cells. Thus, no differences in the average of mean telomere lengths between the two fractions of the 13 patients were found (Table 3).

Inter-clonal kinetic heterogeneity of $CD38^+$ and $CD38^-$ fractions. There were clear differences in $CD38^+$ and $CD38^-$ kinetics among patients (Figure 3). For most of our cases (9/13), defined as Group A (Figure 3A), $CD38^+$ cells rapidly achieved a maximal fraction of ^2H-containing cells at the end of the labeling period. These fractions exceeded, in some instances

dramatically (e.g., CLL 452, 546, and 822), those reached by $CD38^-$ cells. ^2H-incorporation in $CD38^+$ cells then fell during washout. Patient CLL606 was peculiar because of the loss of ^2H-labeled $CD38^-$ cells before the end of the labeling period, although the kinetics for $CD38^+$ cells resemble those observed in the other members of Group A.

However, the kinetics of patients 280, 332, 355 and 625 (Figure 3B, Group B) differed significantly from the 9 patients mentioned above. The fraction of ^2H-labeled $CD38^+$ cells of these patients reached maximum levels only at the end of the washout period. Moreover, $CD38^+$ and $CD38^-$ fractions in these patients had very similar kinetics, compared with the usually clearly divergent and more heterogeneous curves of the other patients.

These observed differences were quantified. The slopes recorded between time point 2 and 3 were concordant positive in Group B and non-concordant positive in Group A (see also Material and Methods).

$CD38^+$ cells may be diluted more rapidly with unlabeled, newly-divided cells during the ^2H_2O washout period. In the presence of decreasing amounts of ^2H, unlabeled $CD38^+$ cells, because of their faster proliferative rate, could more rapidly dilute labeled $CD38^+$ cells than unlabeled $CD38^-$ cells could dilute labeled $CD38^-$ cells. To test this possibility, cells from CLL355, taken when they were maximally enriched in ^2H *in vivo* (Table 2), were loaded with CFSE and stimulated *in vitro* with CpG 2006-G5 plus IL-2 and IL-15; these conditions are known to induce proliferation of human B cells[32]. Four million cells were cultured initially, and a total of 1.8×10^6 cells were recovered at day 5. Based on Annexin V labeling (Figure 4A), 82% of these ($\sim 1.5 \times 10^6$) were scored as viable. These live cells were segregated according to CFSE expression peaks, thereby defining three generations (Figure 4B): generation 0 or

undivided (CFSE mean fluorescence intensity [MFI]: 1600), generation 1 (CFSE MFI: 780) and generation 2 (CFSE MFI: 350). These 3 Annexin V^-CFSE^+ fractions were sorted and analyzed for ^2H-labeled DNA. Enrichment of ^2H in cellular DNA decreased as each new generation arose *in vitro* in the absence of ^2H_2O (Figure 4C). The gated generation 2 probably included a small generation 3 (Figure 4B, dotted lines), thus explaining an MFI and ^2H content lower than the expected reduction from those of generation 1.

Differences in rates at which $CD38^+$ and $CD38^-$ cells leave solid tissues after replication. Differences in ^2H-labeling of $CD38^+$ and $CD38^-$ cells could relate to the time cells take to exit solid tissues where division and ^2H-incorporation into DNA most likely occurred. Because chemokines and their receptors are involved in cell retention, migration, and homing[33-36], we analyzed several chemokine receptors in all 13 patients to determine if a link existed between these receptors and CLL cell kinetics (Figure 5).

CLL cells were evaluated for CCR1, CCR2, CCR4, CCR5, CCR7, CXCR1, CXCR3, CXCR4, and CXCR5, both as percent positive cells as well as MFIs. The latter was necessary because chemokine receptors such as CXCR4, CXCR5 and CCR7 are expressed on virtually every cell in a CLL clone[33], albeit over a range of densities. Only CCR1 and CXCR1 were expressed at greater densities in the $CD38^+$ fractions in all 13 CLL clones studied ($P < 0.05$; Figure 5A).

We then compared data for patients in Group A with those in Group B, since the latter had a slower appearance of ^2H-marked cells in the blood, suggesting longer retention in solid tissues. No differences were found in the percent of chemokine receptor-expressing cells in Group A vs. Group B (not shown).

However, when analyzed for cell surface density, a significant difference for CXCR4 was seen between the two groups (MFI Group B: 720 ± 160 vs. Group A: 238 ± 47; $P = 0.01$; Figure 5B). In addition, all 4 patients in Group B had a CXCR4 MFI higher than 400, compared to only 1/9 in Group A. Furthermore, consistent with the observation that in Group B $CD38^+$ and $CD38^-$ fractions had similar kinetics (Figure 5B), both $CD38^+$ and $CD38^-$ subsets exhibited higher CXCR4 densities compared with the same fractions in Group A (Figure 5C). Thus, higher CXCR4 densities were a property of CLL clones exhibiting delayed appearance in the periphery.

Kinetic patterns of $CD38^+$ and $CD38^-$ subsets relate to clinical outcome. Clinical data for the patients in this report are provided in Table 1. Of the 13 patients studied, 8 experienced progression in Rai stage, required treatment, or had a fatal course. This was the case for all patients in Group B (CLL 280, 332, 355, 625) but only for 4/9 (44.4%) of those in Group A. Group B patients had a shorter, albeit not statistically significant, median time to treatment compared to Group A (57.6 vs. 119.1 months; $P = 0.06$). Also, all Group B patients had involvement of a lymphoid organ detectable by physical examination, while this was the case again for only 4/9 patients of Group A. Mean WBC counts averaged over the course of the study for Group B patients were significantly higher ($P = 0.044$) than those of Group A. Lastly, only one patient (CLL280) in Group B had a leukemic clone expressing a mutated *IGHV*. Among the *IGHV* mutated cases in the entire cohort, CLL280 is the only patient who progressed in terms of a change in Rai stage, had spleen and liver involvement, and the highest WBC and $ZAP\text{-}70^+$ CLL cell counts.

Discussion

In this study we refined our understanding of the proliferative compartment in CLL. We determined that [1] different subsets of cells within a clone divide at different rates, [2] these cells can be identified by surface membrane phenotype, and [3] patients can differ in kinetics of the proliferating subsets. We defined these by measuring ^{2}H-incorporation into genomic DNA, a direct indicator of cell division[22,23] and by focusing on purified populations of cells expressing surface membrane CD38. We chose CD38 because the $CD38^{+}$ subset within CLL clones is enriched in cells that have entered G1[21], and CD38 has biologic relevance and clinical value in the disease[6,15,17].

Using this approach, we found clear evidence for inter- and intra-clonal kinetic heterogeneity. Inter-clonal heterogeneity, based on distinct $CD38^{+}$ and $CD38^{-}$ kinetic patterns, identified two groups of patients, A and B (Figure 3). In Group A cases (9/13 subjects), the fraction of ^{2}H-labeled $CD38^{+}$ cells rose quickly to plateau levels and then declined, whereas the fraction of labeled $CD38^{-}$ cells rose slowly to a maximum and declined at a slower rate during washout such that the $CD38^{+}$ and $CD38^{-}$ washout curves often intersected (Figure 3A). Conversely, in Group B patients, $CD38^{+}$ and $CD38^{-}$ cells displayed similar kinetics, with continuous increases in the fraction of ^{2}H-labeled cells throughout study periods, including the washout phase (Figure 3B). After $^{2}H_2O$ has washed out, label is no longer available to mark subsequently born cells. Therefore, if there is a continued increase in the percent labeled cells in the circulation during the washout period, this must represent a release of previously labeled/divided cells from the extra-vascular space.

We also identified intra-clonal heterogeneity. In every patient a larger enrichment of newly-produced $CD38^{+}$ than $CD38^{-}$ cells was found during the period when $^{2}H_2O$ was present in

body water (Table 2). This was evident throughout the labeling period for both Group A and B patients and persisted at the end of labeling in Group B. Importantly, the higher fraction of newly-divided cells was a general characteristic of the $CD38^+$ compartment, regardless of the percent of $CD38^+$ cells present in a leukemic clone (range: 1 - 98%; Table 1). However in Group A patients, we observed a decrease in the percentage of $CD38^+$, ^2H-labeled cells, which in 4 cases (CLL189, 321, 569, and 822) was paralleled by an increase in the percentage of $CD38^-$ labeled cells (Table 2).

Loss of circulating $CD38^+$, ^2H-labeled cells after ceasing ^2H_2O intake can be explained by different, not mutually exclusive mechanisms.

1. Higher death rates of rapidly proliferating cells. Cell death of activated, proliferating T and B cells occurs[37,38], thereby maintaining steady-state cell numbers over time. In studies of T-cell kinetics using ^2H incorporation, this mechanism can explain why curves of appearance and disappearance of labeled cells have similar slopes[39]. Thus decay of labeled $CD38^+$ cells, characteristically observed in Group A patients (Figure 3A), could indicate higher death rates of the more proliferative fraction.

2. Change in surface membrane phenotype over time with some $CD38^+$ cells becoming $CD38^-$. In 4/9 Group A patients, decay of $CD38^+$, ^2H-labeled cells was paralleled by an increase in $CD38^-$ labeled cells (Figure 3A and Table 2). For example, for CLL822, between the end of labeling and end of washout, the *f* of ^2H-labeled $CD38^+$ cells decreased ~50% (44% to 20.8%), while the *f* of labeled $CD38^-$ increased by ~15% (11% to 13%; Table 2). These reciprocal changes may indicate that a portion of $CD38^+$ cells became $CD38^-$, and the remaining either died or left the circulation and were retained in a solid tissue, thereby becoming undetectable.

Such a phenotypic conversion of some $CD38^+$ cells is also suggested by experiments with sorted Ki-67^+CD38^+ and Ki-67^+CD38^- cells (Figure 2 and Table 2). These fractions tended to equalize in terms of newly-divided cells (Figure 2B and C), due either to (a) an early equilibration of ^2H-labeled cells among the two compartments as a result of proliferating $CD38^+$ cells becoming $CD38^-$ or (b) $CD38^+$Ki-67^+ and $CD38^-$Ki-67^+ fractions constituting two distinct compartments proliferating at very similar (but different) rates. We favor the first explanation, for at least the majority of $CD38^+$ fractions. In fact, if $CD38^+$ and $CD38^-$ were two distinct compartments and the $CD38^+$ compartment proliferated more rapidly the percentage of $CD38^+$ cells within a clone would increase at the end of washout or over longer periods of time (unless all newly-divided cells died). Although the percentage of $CD38^+$ cells within a clone can change, it is not common (refs.[6,40] and Supplemental Figure 1). Moreover, if $CD38^+$ and $CD38^-$ cells were distinct stable subgroups, $CD38^+$ cells should exhibit features of longer proliferative histories. However, this was not the case because mean telomere lengths were similar among $CD38^+$ and $CD38^-$ cells of each clone (Table 3 and refs.[21,41]). These findings support the concept that at least a portion of the $CD38^+$ and $CD38^-$ fractions is a *continuum* of the same cell population.

In this regard, two recent intra-clonal comparisons of chromosomal aberrations in $CD38^+$ and $CD38^-$ fractions reached different conclusions, one in support and one against a change of CD38 phenotype (refs. [42,43]; note that the latter reference includes 4 patients enrolled in this study – CLL 355, 452, 625, and 931). If the phenotype of all $CD38^+$ cells could change overtime, similar chromosomal aberrations should exist in each fraction. However, if such a transition occurred in only a fraction of $CD38^+$ cells and the size of this fraction differed among patients, then genomic changes might prevail in one fraction and not another; in such a situation, detection

of these differences would depend on the size of a fraction and the sensitivity of the method measuring genomic aberrations. Our kinetic data provide indications of clonal heterogeneity, the extent of which is still not known but that might explain these apparent inconsistencies.

3. Dilution of a labeled population by unlabeled cells when proliferation occurs in absence of ^2H_2O. When labeled CLL cells proliferated *ex vivo* in the absence of ^2H_2O, ^2H content among daughter cells decreased with each generation (Figure 5). This was likely due to the production of newly-synthesized DNA in the absence of ^2H, thereby "diluting" labeled DNA by unlabeled DNA (Figure 5C). Thus, at least a part of the decay curve for $CD38^+$ cells is due to ongoing proliferation in the absence of ^2H_2O. This phenomenon would have a greater effect in the population that proliferates faster, i.e., the $CD38^+$ subset.

4. Differential rates of entering and leaving the blood from solid lymphoid tissues. In humans, BrdU-labeled T cells equilibrate between blood and lymphoid tissues within 24 hours[44]. The same rapid equilibration was not found for proliferating B cells; in fact, there were 6 times higher numbers in lymphoid tissues than blood at all time points considered[44]. *In vivo* rates of CLL cells flowing from peripheral blood into solid lymphoid tissues and vice versa are poorly understood, although a few studies have attempted to dissect the former trafficking[45-47].

In regards the latter situation, $CD38^-$ cells in every patient except CLL931 reached plateaus later than $CD38^+$ cells (Figure 3A and B). This could represent differences in activation states and in chemokine receptor expression between the two subpopulations. Indeed, higher levels of CCR1 and CXCR1 were found among $CD38^+$ cells (Figure 5A), probably due to a more activated state of this proliferating population. CCR1 is over-expressed on normal B cells activated *in vitro*[48]; this issue has not been addressed directly for CXCR1.

In addition, a relationship between CLL cell kinetics and CXCR4 levels was found between Group A and Group B patients (Figure 5B and C). In this inter-clonal comparison, delayed appearance of labeled cells in Group B suggested longer retention within lymphoid tissues. Consistent with this idea, Group B clones had significantly higher densities of surface membrane CXCR4 compared to Group A. Longer retention in solid tissues would give cells a prolonged exposure to survival factors and stimulatory ligands, and CXCR4 may have a crucial role in regulating this process[25,26]. Proliferation centers are characteristically found in solid lymphoid tissues of patients, and it appears that leukemic cell proliferation and CD38 up-regulation occurs within these structures[49]. Our observed proliferation rates, together with CXCR1 and CCR1 expression levels, suggest that $CD38^+$ cells have more recently left a solid tissue where they proliferated, either spontaneously or after receiving activating stimuli. Within each clone, moreover, the fraction expressing lower levels of surface CXCR4 was enriched in $CD38^+$ cells and $CD5^+$ cells and incorporated more ^2H than the fraction with higher levels of CXCR4 (manuscript in preparation). These findings also support a model in which, within the context of a lymphoid solid tissue, CLL cells down modulate CXCR4 (following CXCL12/SDF-1 ligation and activation stimuli) and ornate cell membranes with more CD38 and CD5.

Remarkably, and in line with the relationship between CXCR4 expression, bone marrow infiltration, and Rai stage[50], all Group B patients experienced disease progression, regardless of *IGHV* mutation status (Table 1). Of interest, an *in vivo* study performed in the 1960s analyzing CLL cell kinetics using ^3H-thymidine incorporation[45] described two groups of patients: Group 1 in which labeled cells rapidly peaked and then disappeared (similar to our Group A) and Group 2 with a flat slope of labeled cells (similar to Group B). In that study, Group 2 patients had more organomegaly and higher WBC counts. In line with this, all Group B patients had lymphoid

organ involvement compared to 4/9 Group A patients. Furthermore, Group B patients had a shorter time to treatment (57.6 vs. 119.1 months) and higher WBC counts than Group A patients. Thus, differences in CXCR4 levels between leukemic clones relates well to differences in CLL cell kinetics and possibly clinical outcome.

A relationship between CLL kinetics, based on ^{2}H-incorporation, and disease activity was previously suggested, with higher birth rates associating with more aggressive disease[3]. In addition, higher numbers of CD38-expressing cells correlate with greater risk of a poor clinical course and shortened survival[6]. Since DNA replication is a pre-requisite for the accumulation of new DNA lesions that could result in disease progression, our data suggest a link between percent of $CD38^{+}$ cells and clinical deterioration and outcome. Surprisingly, however, a clear correlation between the percentage of $CD38^{+}$ proliferating cells in CLL clones and disease progression and survival was not found. Further studies with additional patients will be necessary to test this link.

In summary, this study demonstrates both intra- and inter-clonal heterogeneity in the proliferation of CLL cells. Some of this heterogeneity may be specious but still important, resulting from changes in surface membrane phenotype and differences in proliferative rates between the $CD38^{+}$ and $CD38^{-}$ fractions in the absence of $^{2}H_2O$. Other heterogeneity likely reflects fundamental differences in CLL subset survival and trafficking, e.g., CXCR4 expression. Therefore, classifying patients on the basis of differences in CLL cell kinetics (e.g., Group A vs. B) can reveal molecular differences in leukemic cells and may eventually pinpoint differential balances between pro-survival, proliferative and apoptotic mechanisms within solid tissues. Combining the ^{2}H-labeling approach with more extensive cell surface and genetic analyses may help to further dissect these complexities. Indeed, a refined definition of the CLL proliferative

compartment might allow us to focus our therapeutic strategies on the aggressive core of the clone and possibly identify leukemic stem cells in CLL, should they exist.

Acknowledgments

We thank the FACS core facility at The Feinstein Institute for Medical Research for technical help. This study was supported in part by grants from the CLL Global Research Foundation, Houston, TX, and the National Center for Research Resources of the NIH (M01 General Clinical Research Center Grant, RR018535). In addition, The Karches Foundation, The Prince Foundation, The Marks Foundation, The Jerome Levy Foundation, The Leon Levy Foundation, The Tebil Foundation, Inc., and Joseph Eletto Leukemia Research Fund provided support.

Authorship contribution

C.C. performed research, analyzed data and wrote the paper, R.N.D. assisted with the experiments and reviewed work, G.H., E.J.M and M.K.H. performed Gas Chromatography/Mass Spectrometry analyses and reviewed the paper, C.S. contributed analytical tools, M.S.K., J.E.K., S.L.A. and K.K.R. coordinated the clinical work, N.C. designed research and wrote the paper.

Conflict of interest disclosure

M.K.H.: ownership interest in KineMed, Inc.

G.H., E.J.M., N.C.: stock options in KineMed, Inc.

References

1. Chiorazzi N, Rai KR, Ferrarini M. Chronic Lymphocytic Leukemia. *N Engl J Med*. 2005;352(8):804-815.
2. Ferrarini M, Chiorazzi N. Recent advances in the molecular biology and immunobiology of chronic lymphocytic leukemia. *Semin Hematol*. 2004;41(3):207-223.
3. Messmer BT, Messmer D, Allen SL, et al. In vivo measurements document the dynamic cellular kinetics of chronic lymphocytic leukemia B cells. *J Clin Invest*. 2005;115(3):755-764.
4. Caligaris-Cappio F. Biology of chronic lymphocytic leukemia. *Rev Clin Exp Hematol*. 2000;4(1):5-21.
5. Ghia P, Caligaris-Cappio F. The indispensable role of microenvironment in the natural history of low-grade B-cell neoplasms. *Adv Cancer Res*. 2000;79157-173.
6. Damle RN, Wasil T, Fais F, et al. Ig V gene mutation status and CD38 expression as novel prognostic indicators in chronic lymphocytic leukemia. *Blood*. 1999;94(6):1840-1847.
7. Hamblin TJ, Davis Z, Gardiner A, Oscier DG, Stevenson FK. Unmutated Ig VH genes are associated with a more aggressive form of chronic lymphocytic leukemia. *Blood*. 1999;94(6):1848-1854.
8. Fais F, Ghiotto F, Hashimoto S, et al. Chronic lymphocytic leukemia B cells express restricted sets of mutated and unmutated antigen receptors. *J Clin Invest*. 1998;102(8):1515-1525.

9. Crespo M, Bosch F, Villamor N, et al. ZAP-70 expression as a surrogate for immunoglobulin-variable-region mutations in chronic lymphocytic leukemia. *N Engl J Med*. 2003;348(18):1764-1775.

10. Wiestner A, Rosenwald A, Barry TS, et al. ZAP-70 expression identifies a chronic lymphocytic leukemia subtype with unmutated immunoglobulin genes, inferior clinical outcome, and distinct gene expression profile. *Blood*. 2003;101(12):4944-4951.

11. Ghia P, Guida G, Stella S, et al. The pattern of CD38 expression defines a distinct subset of chronic lymphocytic leukemia (CLL) patients at risk of disease progression. *Blood*. 2003;101(4):1262-1269.

12. Mehta K, Shahid U, Malavasi F. Human CD38, a cell-surface protein with multiple functions. *Faseb J*. 1996;10(12):1408-1417.

13. Ferrero E, Malavasi F. Human CD38, a leukocyte receptor and ectoenzyme, is a member of a novel eukaryotic gene family of nicotinamide adenine dinucleotide+-converting enzymes: extensive structural homology with the genes for murine bone marrow stromal cell antigen 1 and aplysian ADP-ribosyl cyclase. *J Immunol*. 1997;159(8):3858-3865.

14. Deaglio S, Capobianco A, Bergui L, et al. CD38 is a signaling molecule in B-cell chronic lymphocytic leukemia cells. *Blood*. 2003;102(6):2146-2155.

15. Deaglio S, Vaisitti T, Aydin S, Ferrero E, Malavasi F. In-tandem insight from basic science combined with clinical research: CD38 as both marker and key component of the pathogenetic network underlying chronic lymphocytic leukemia. *Blood*. 2006;108(4):1135-1144.

16. Pascual V, Liu YJ, Magalski A, de Bouteiller O, Banchereau J, Capra JD. Analysis of somatic mutation in five B cell subsets of human tonsil. *J Exp Med*. 1994;180(1):329-339.

17. Deaglio S, Vaisitti T, Bergui L, et al. CD38 and CD100 lead a network of surface receptors relaying positive signals for B-CLL growth and survival. *Blood*. 2005;105(8):3042-3050.

18. Pepper C, Ward R, Lin TT, et al. Highly purified CD38(+) and CD38(-) sub-clones derived from the same chronic lymphocytic leukemia patient have distinct gene expression signatures despite their monoclonal origin. *Leukemia*. 2007;21(4):687-696.

19. Aydin S, Rossi D, Bergui L, et al. CD38 gene polymorphism and chronic lymphocytic leukemia: a role in transformation to Richter's syndrome? *Blood*. 2008blood-2008-2001-129726.

20. Zucchetto A, Benedetti D, Tripodo C, et al. CD38/CD31, the CCL3 and CCL4 chemokines, and CD49d/vascular cell adhesion molecule-1 are interchained by sequential events sustaining chronic lymphocytic leukemia cell survival. *Cancer Res*. 2009;69(9):4001-4009.

21. Damle RN, Temburni S, Calissano C, et al. CD38 expression labels an activated subset within chronic lymphocytic leukemia clones enriched in proliferating B cells. *Blood*. 2007;110(9):3352-3359.

22. Busch R, Neese RA, Awada M, Hayes GM, Hellerstein MK. Measurement of cell proliferation by heavy water labeling. *Nat Protoc*. 2007;2(12):3045-3057.

23. Neese RA, Misell LM, Turner S, et al. Measurement in vivo of proliferation rates of slow turnover cells by 2H2O labeling of the deoxyribose moiety of DNA. *Proc Natl Acad Sci U S A*. 2002;99(24):15345-15350.

24. van Gent R, Kater AP, Otto SA, et al. In vivo Dynamics of Stable Chronic Lymphocytic Leukemia Inversely Correlate with Somatic Hypermutation Levels and Suggest No Major Leukemic Turnover in Bone Marrow. *Cancer Res*. 2008;68(24):10137-10144.

25. Burger JA, Burger M, Kipps TJ. Chronic lymphocytic leukemia B cells express functional CXCR4 chemokine receptors that mediate spontaneous migration beneath bone marrow stromal cells. *Blood*. 1999;94(11):3658-3667.

26. Burger JA, Kipps TJ. CXCR4: a key receptor in the crosstalk between tumor cells and their microenvironment. *Blood*. 2006;107(5):1761-1767.

27. Cheson BD, Bennet JM, Grever M, et al. National Cancer Institute-sponsored working group guidelines for chronic lymphocytic leukemia: revised guidelines for diagnosis and treatment. *Blood*. 1996;87(12):4990-4997.

28. Chen JL, Peacock E, Samady W, et al. Physiologic and pharmacologic factors influencing glyceroneogenic contribution to triacylglyceride glycerol measured by mass isotopomer distribution analysis. *J Biol Chem*. 2005;280(27):25396-25402.

29. Damle RN, Batliwalla FM, Ghiotto F, et al. Telomere length and telomerase activity delineate distinctive replicative features of the B-CLL subgroups defined by immunoglobulin V gene mutations. *Blood*. 2004;103(2):375-382.

30. Brown DC, Gatter KC. Ki67 protein: the immaculate deception? *Histopathology*. 2002;40(1):2-11.

31. Damle R, Allen S, Rai KR, Chiorazzi N. CD38 expression identifies an active subset of proliferating cells within the clonal population in chronic lymphocytic leukemia patients (in vitro analysis). *Blood*. 2006;108(11):13a.

32. Darce JR, Arendt BK, Chang SK, Jelinek DF. Divergent Effects of BAFF on Human Memory B Cell Differentiation into Ig-Secreting Cells. *J Immunol*. 2007;178(9):5612-5622.

33. Lopez-Giral S, Quintana NE, Cabrerizo M, et al. Chemokine receptors that mediate B cell homing to secondary lymphoid tissues are highly expressed in B cell chronic lymphocytic leukemia and non-Hodgkin lymphomas with widespread nodular dissemination. *J Leukoc Biol*. 2004;76(2):462-471.

34. Cyster JG. Chemokines and cell migration in secondary lymphoid organs. *Science*. 1999;286(5447):2098-2102.

35. Okada T, Ngo VN, Ekland EH, et al. Chemokine requirements for B cell entry to lymph nodes and Peyer's patches. *J Exp Med*. 2002;196(1):65-75.

36. Ansel KM, Ngo VN, Hyman PL, et al. A chemokine-driven positive feedback loop organizes lymphoid follicles. *Nature*. 2000;406(6793):309-314.

37. Renno T, Attinger A, Locatelli S, Bakker T, Vacheron S, MacDonald HR. Cutting edge: apoptosis of superantigen-activated T cells occurs preferentially after a discrete number of cell divisions in vivo. *J Immunol*. 1999;162(11):6312-6315.

38. Mongini PKA, Inman JK, Han H, Kalled SL, Fattah RJ, McCormick S. Innate Immunity and Human B Cell Clonal Expansion: Effects on the Recirculating B2 Subpopulation. *J Immunol*. 2005;175(9):6143-6154.

39. Macallan DC, Asquith B, Irvine AJ, et al. Measurement and modeling of human T cell kinetics. *Eur J Immunol*. 2003;33(8):2316-2326.

40. Hamblin TJ, Orchard JA, Ibbotson RE, et al. CD38 expression and immunoglobulin variable region mutations are independent prognostic variables in chronic lymphocytic leukemia, but CD38 expression may vary during the course of the disease. *Blood*. 2002;99(3):1023-1029.

41. Pepper C, Brennan P, Alghazal S, et al. CD38+ chronic lymphocytic leukaemia cells co-express high levels of ZAP-70 and are functionally distinct from their CD38- counter-parts. *Leukemia*. 2006;20(4):743-744.

42. Lin TT, Hewamana S, Ward R, et al. Highly purified CD38 sub-populations show no evidence of preferential clonal evolution despite having increased proliferative activity when compared with CD38 sub-populations derived from the same chronic lymphocytic leukaemia patient. *Br J Haematol*. 2008;142(4):595-605.

43. Grubor V, Krasnitz A, Troge JE, et al. Novel genomic alterations and clonal evolution in chronic lymphocytic leukemia revealed by representational oligonucleotide microarray analysis (ROMA). *Blood*. 2009;113(6):1294-1303.

44. Kovacs JA, Lempicki RA, Sidorov IA, et al. Identification of dynamically distinct subpopulations of T lymphocytes that are differentially affected by HIV. *J Exp Med*. 2001;194(12):1731-1741.

45. Zimmerman TS, Godwin HA, Perry S. Studies of leukocyte kinetics in chronic lymphocytic leukemia. *Blood*. 1968;31(3):277-291.

46. Stryckmans PA, Debusscher L, Collard E. Cell kinetics in chronic lymphocytic leukaemia (CLL). *Clin Haematol*. 1977;6(1):159-167.

47. Dormer P, Theml H, Lau B. Chronic lymphocytic leukemia: a proliferative or accumulative disorder? *Leuk Res*. 1983;7(1):1-10.

48. Corcione A, Tortolina G, Bonecchi R, et al. Chemotaxis of human tonsil B lymphocytes to CC chemokine receptor (CCR) 1, CCR2 and CCR4 ligands is restricted to non-germinal center cells. *Int Immunol*. 2002;14(8):883-892.

49. Patten PE, Buggins AG, Richards J, et al. CD38 expression in chronic lymphocytic leukemia is regulated by the tumor microenvironment. *Blood*. 2008;111(10):5173-5181.

50. Ghobrial IM, Bone ND, Stenson MJ, et al. Expression of the chemokine receptors CXCR4 and CCR7 and disease progression in B-cell chronic lymphocytic leukemia/ small lymphocytic lymphoma. *Mayo Clin Proc*. 2004;79(3):318-325.

Table 1. Clinical and laboratory features of the CLL patients involved in this study

na: Data not available

	% CD38^{+}	% ZAP-70^{+}	Cytogenetic abnormalities (% cells)				*IGHV* mutation status[A]	Lymph node/Spleen/Liver enlargement [B]	Rai stage at diagnosis and when $^{2}H_{2}O$ study began	Status	Time to first treatment (months)[C]	Mean WBC (beginning, end o study)
			Δ11q22	Tri12	Δ13q14	Δ17p23						
CLL189	2	7	<5	<5	70	<5	M/UM	+ / - / -	0-IV	Expired	53	107 (76-175)
CLL280	1	29	<5	<5	99	<5	M	- / + / +	0-II	Alive	108	58 (61-75)
CLL321	10	95	<5	59	<5	<5	UM	- / - / -	0-0	Alive	None	73 (102-80)
CLL332	66	88	na	<5	93.5	<5	UM	+ / - / -	I-I	Alive	28	74 (na-83)
CLL355	25	18	68	<5	25	<5	UM	+ / - / -	I-I	Expired	88	228 (71-310)
CLL452	36	48	na	na	na	na	M/UM	+ / - / -	0-I	Alive	36	79 (63-125)
CLL546	7	6	0	0	78	0	M	- / - / -	0-0	Alive	None	32 (27-35)
CLL569	98	40	0	0	0	0	UM	- / +/ -	II-II	Alive	None	73 (52-95)
CLL606	8	5	0	0	68	0	M	- / - / -	0-0	Alive	None	29 (30-35)
CLL625	54	57	80	0	0	0	UM	++ / - / -	II-II	Alive	17	297 (245-361)
CLL822	22	56	0	0	na	0	UM	- / + / -	0-III	Alive	108	43 (30-29)
CLL875	14	18	0	0	0	0	M	- / - / -	0-0	Alive	None	15 (15-15)
CLL931	63	49	na	na	na	na	UM	- / - / -	0-0	Expired	None	20 (17-28)

[A] ≤ 2% difference from the germline gene defines a patient as *IGHV* unmutated (UM); >2% difference defines a patient as *IGHV* mutated (M).

[B] Lymph nodes: + 1 - 1.5 cm; ++ 1.5 - 3 cm. + for spleen and liver defines them as palpable by physical examination or enlarged on imaging (ultrasound or CT scan). Only data 6 months before or after the study are included.

[C] Time from initial diagnosis to first treatment for clinical progression of CLL.

[D] Mean WBC count recorded during $^{2}H_{2}O$ protocol period; in brackets are values at the beginning and end of the protocol.

Note that WBC data for CLL569 were incomplete (only beginning and end values were available) and WBC count of CLL332 at the beginning of the study was not available

.

Table 2

Fraction (%) of $CD38^+$ and $CD38^-$ ^2H-labeled cells (*f*) in the clones of CLL patients involved in this study

	1st Time Point			2nd Time Point			3rd Time Point		
CLL	$CD38^+$(*f*)	$CD38^-$ (*f*)	$CD38^+$(*f*) / $CD38^-$ (*f*)	$CD38^+$(*f*)	$CD38^-$ (*f*)	$CD38^+$(*f*) / $CD38^-$ (*f*)	$CD38^+$(*f*)	$CD38^-$ (*f*)	$CD38^+$(*f*) / $CD38^-$ (*f*)
189	30.0	17.0	1.8	31.0	26.0	1.2	24.0	29.0	0.8
280	7.5	8.5	0.9	15.6	12.0	1.3	16.9	12.6	1.3
321	19.5	14.1	1.4	26.5	19.2	1.4	20.4	22.5	0.9
332	2.4	1.5	1.6	3.2	2.1	1.5	16.0	14.0	1.1
355	2.1	1.9	1.1	8.9	7.3	1.2	26.6	21.3	1.2
452	16.0	2.7	5.9	25.0	8.4	3.0	9.1	7.3	1.2
546	28.0	4.7	5.9	34.4	10.7	3.2	10.7	9.5	1.1
569	24.0	8.7	2.8	40.7	16.3	2.5	21.7	21.0	1.0
606	46.2	22.1	2.8	73.3	8.9	8.2	4.8	5.1	0.9
625	1.8	1.5	1.2	9.7	6.4	1.5	13.4	10.0	1.3
822	26.5	5.3	5.0	44.0	11.0	4.0	20.8	13.3	1.6
875	3.6	1.8	2.0	6.6	5.3	1.2	4.7	5.0	0.9
931	8.7	3.3	2.6	18.4	12.1	1.5	8.1	7.5	1.1
Avg	**16.5 ± 3.9[A]**	**7.3 ± 1.8[A]**	**2.7 ± 0.5**	**25.9 ± 5.4[B]**	**11.2 ± 1.7[B]**	**2.4 ± 0.5**	**15.2 ± 2[C]**	**13.7 ± 2.1[C]**	**1.1 ± 0.1**

Paired t-test: [A] $P < 0.01$, [B] $P = 0.013$, [C] $P = 0.25$

Table 3

Mean telomere lengths (kilobases) measured in

$CD19^+CD5^+$, $CD19^+CD5^+CD38^+$and $CD19^+CD5^+CD38^-$ fractions

CLL	$CD19^+$	$CD38^+$	$CD38^-$
189	6.61	5.18	4.75
280	5.16	8.76	4.17
321	4.7	4.23	3.76
332	0.56	0.99	0.9
355	3.72	3.31	4.51
452	1.19	1.11	2.13
546	7.54	8.27	8.04
569	2.35	2.79	1.39
606	3.64	3.22	3.4
625	1.94	2.11	1.19
822	2.76	2.72	4.48
875	3.77	4.02	3.74
931	4.16	3.89	4.34
mean	**3.7 ± 0.56**	**3.9 ± 0.66**	**3.6 ± 0.53**

Figure Legends

Figure 1. Procedure for determining ^2H enrichments in $CD38^+$ and $CD38^-$ CLL cells and time point selection in relation to ^2H availability in body water.

A. Deuterium enrichment measured in plasma of body water compartment of a representative case (CLL875). CLL cells were flow-sorted at the 3 time points indicated by arrows. Vertical dashed line indicates time when ^2H_2O intake was ended.

B. After gating $CD19^+CD3^-$ cells, $CD5^+$ cells were flow sorted based on their expression of CD38. ^2H in genomic DNA was then measured by GC/MS.

C. The ratio of $CD38^+/CD38^-$ fractions (*f*) of labeled cells (Table 2) was averaged. Bars represent each of the 3 time points studied. Significant differences in ^2H incorporation between the $CD38^-$ and $CD38^+$ B-CLL subpopulations were achieved early and maintained during labeling period, whereas they disappeared during washout.

Figure 2. CD38 expression in $Ki67^+$ and $Ki67^-$ CLL cells and ^2H enrichment in CLL clonal fractions sorted based on CD38 and Ki67.

A. PBMCs from CLL822 were incubated with fluorochrome-labeled mAbs reactive with CD19, CD5, and CD38, and, after cell permeabilization, with Ki67. Cells were first gated for CD19 and then analyzed as reported in the figure. **Upper plot:** CLL clone contains ~5% $Ki67^+$ cells. **Lower plots:** Percent of $CD38^+$ cells in the $CD19^+CD5^+Ki67^+$ fraction (83%; lower right) is much higher compared to that observed in the $CD19^+CD5^+Ki67^-$ fraction (18%; lower left).

B-C. CLL cells from CLL452 (B) and CLL625 (C) were flow-sorted based on CD38 and Ki67 expression, and ^2H-labeled DNA was measured in the sorted fractions. Curves represent

the fraction (*f*) of labeled cells reported in the Tables. $Ki67^+$ cells, both $CD38^-$ and $CD38^+$, incorporated more ^2H than their $Ki67^-$ counterparts.

Figure 3. Kinetics of $CD38^+$ and $CD38^-$ CLL cells in each patient studied.

Curves represent the fraction (*f*) of labeled cells at the 3 time points studied. Note that different levels of ^2H enrichment were observed among patients, and the graphs have different scales. Vertical dotted lines indicate the end of ^2H_2O assumption. Based on the slopes of the $CD38^+$ and $CD38^-$ kinetic curves, two groups of patients were defined, A and B.

A. In Group A, $CD38^+$ cells rapidly achieve maximal ^2H enrichment levels at the end of the labeling period; ^2H incorporation in these cells subsequently falls during washout.

B. Patients in Group B are characterized by similar kinetic patterns of both $CD38^+$ and $CD38^-$ fractions with delayed appearance and slow achievement of maximal levels of labeled cells.

Figure 4. ^2H content decreases generation after generation among cells that proliferate in absence of ^2H_2O.

A. PBMCs from CLL355 at the third time point during ^2H_2O protocol (Table 2) were loaded with CFSE and cultured with CpG 2006-G5 (5μg/ml), IL2 (5ng/ml) and IL15 (5ng/ml) to induce proliferation. Cells were harvested after 5 days and stained with Annexin V-APC to exclude dying/dead cells.

B. Annexin V^- cells were analyzed for CFSE content and three generations of cells were flow-sorted based on the indicated gates (0, 1, 2). Gate 0 represents undivided cells. Note that while gate 0 and 1 contained discreet CFSE peaks, gate 2 probably contained a main peak and a smaller one (dotted lines), possibly representing another generation of progeny.

C. A decreased fraction (*f*) of labeled cells was found generation after generation.

Figure 5. Chemokine receptor levels on CLL cells of patients in the study.

Surface membrane expression of a panel of chemokine receptors was evaluated in the 13 patients in the study. All the samples were analyzed in the same experiment.

A. Of the chemokine receptor levels studied (see text for the list), only two (CCR1 and CXCR1) were expressed at significantly higher densities (MFI) in $CD38^+$ compared to $CD38^-$ cells ($P < 0.05$).

B. Group B patients (n = 4) had significantly higher CXCR4 levels (MFI) compared to Group A (n = 9; $P = 0.01$). Comparisons of the other chemokine receptors revealed no significant differences between the two groups.

C. Both $CD38^+$ (left) and $CD38^-$ (right) fractions from Group B patients exhibited significantly higher CXCR4 levels compared to the same fractions from Group A ($P = 0.02$).

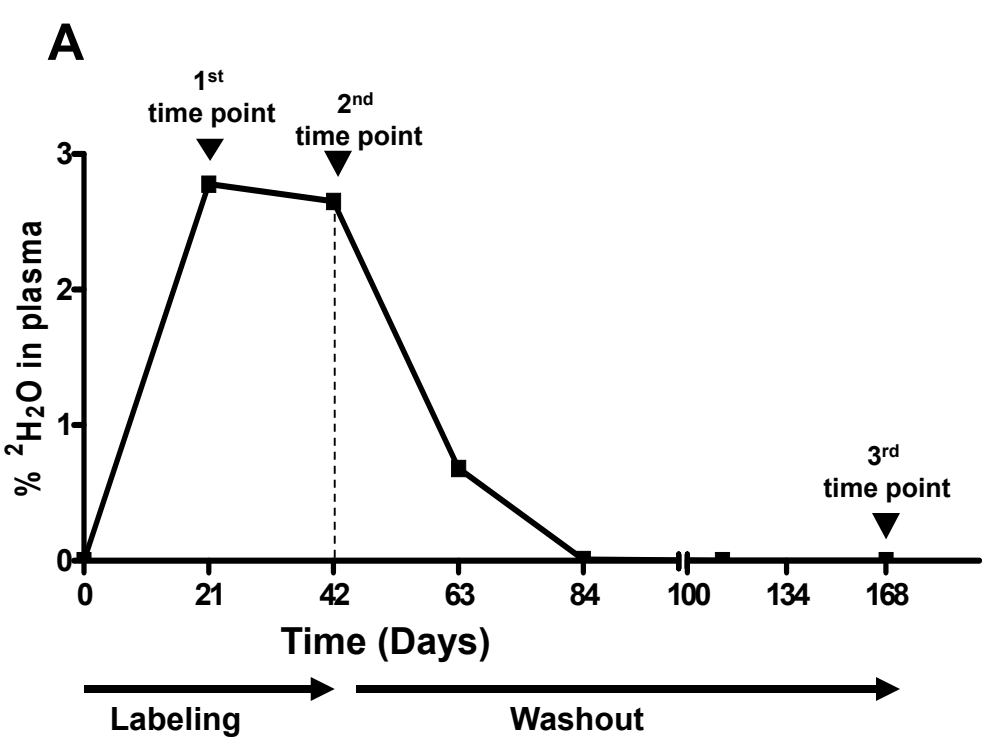

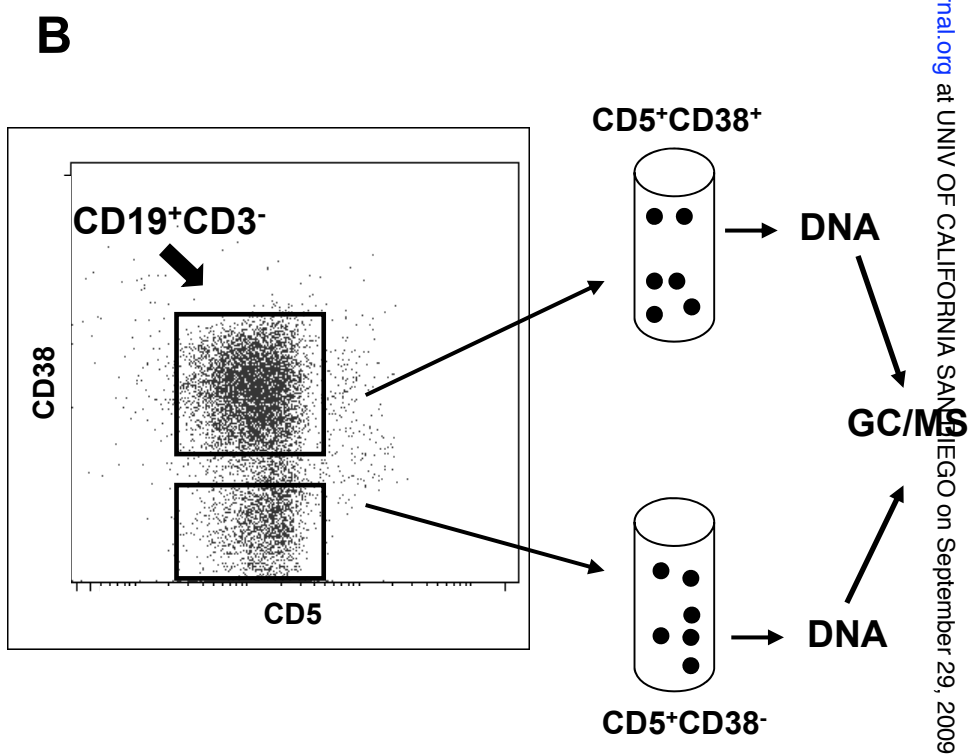

Calissano *et al.* Fig. 1

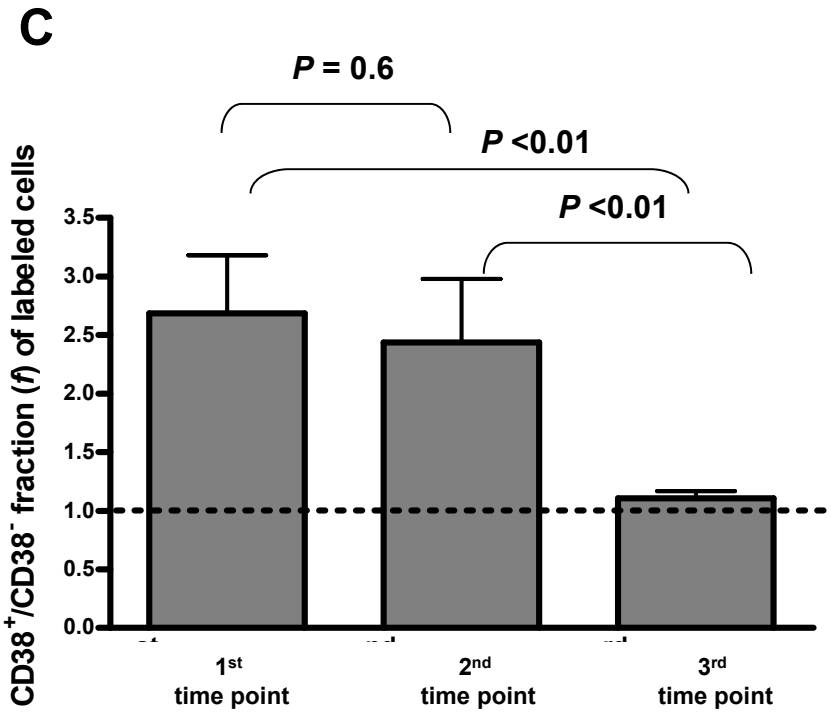

Calissano *et al.* Fig. 2

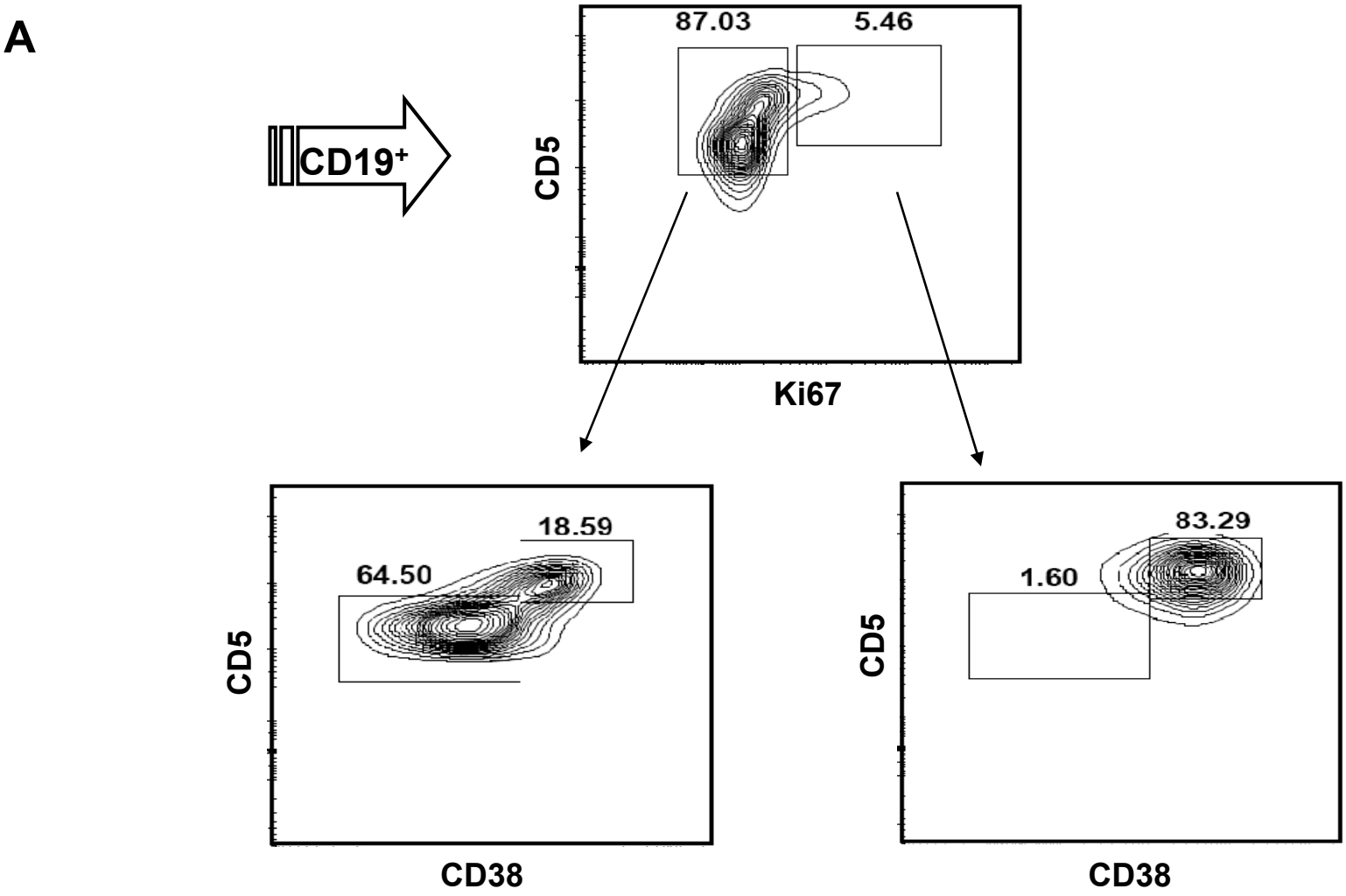

B

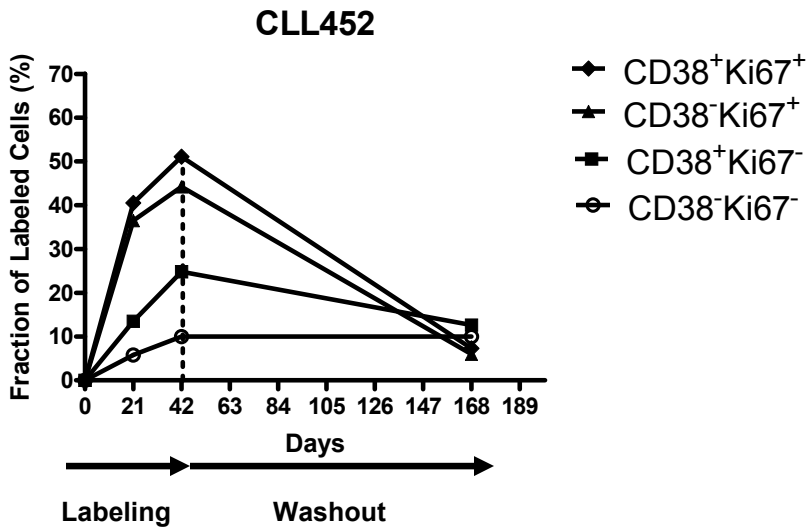

Days	$CD38^-Ki67^-$	$CD38^-Ki67^+$	$CD38^+Ki67^-$	$CD38^+Ki67^+$
0	0.0%	0.0%	0.0%	0.0%
21	5.8%	36.5%	13.5%	40.5%
42	10.0%	44.2%	24.8%	51.1%
168	10.0%	6.0%	12.6%	7.3%

C

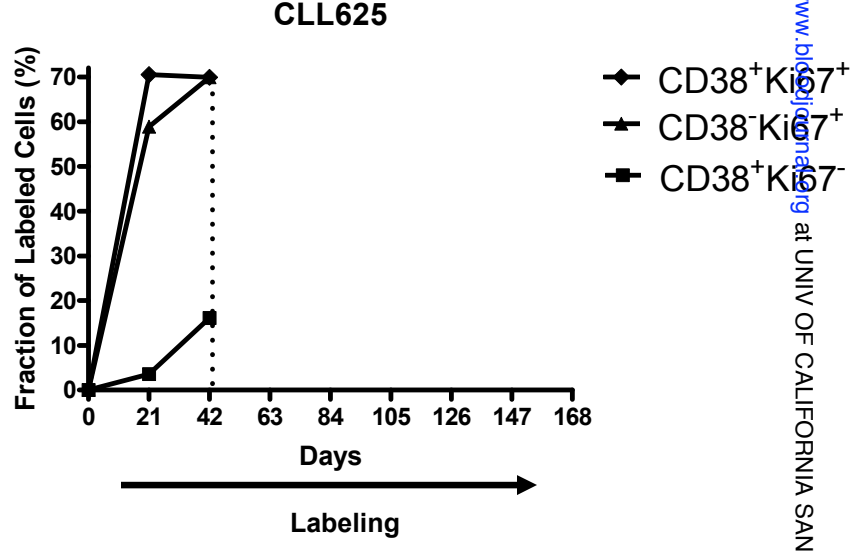

Days	$CD38^-Ki67^+$	$CD38^+Ki67^-$	$CD38^+Ki67^+$
0	0.0%	0.0%	0.0%
21	58.9%	3.6%	70.5%
42	69.9%	16.1%	69.9%

Calissano *et al.* Fig. 3

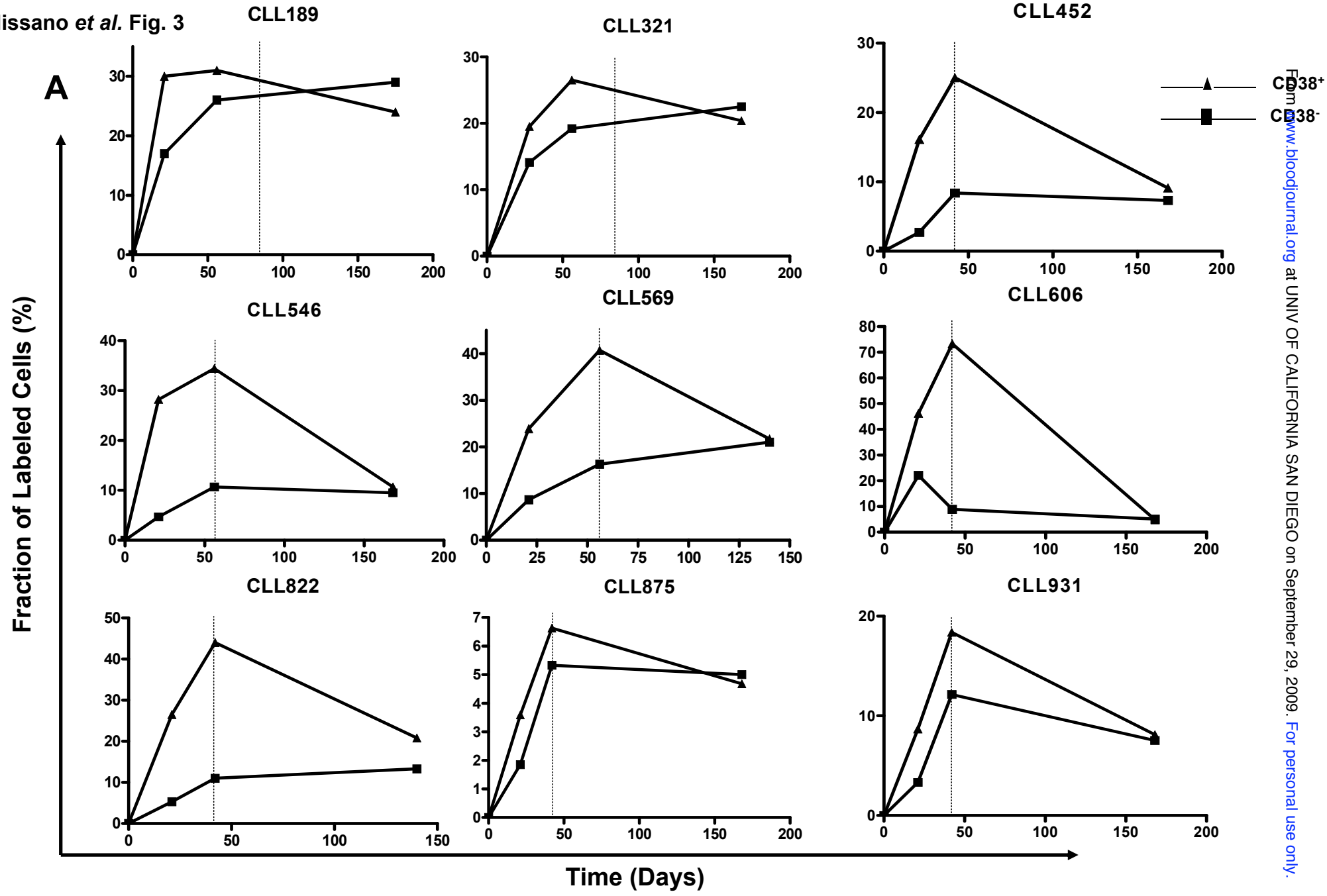

Group A

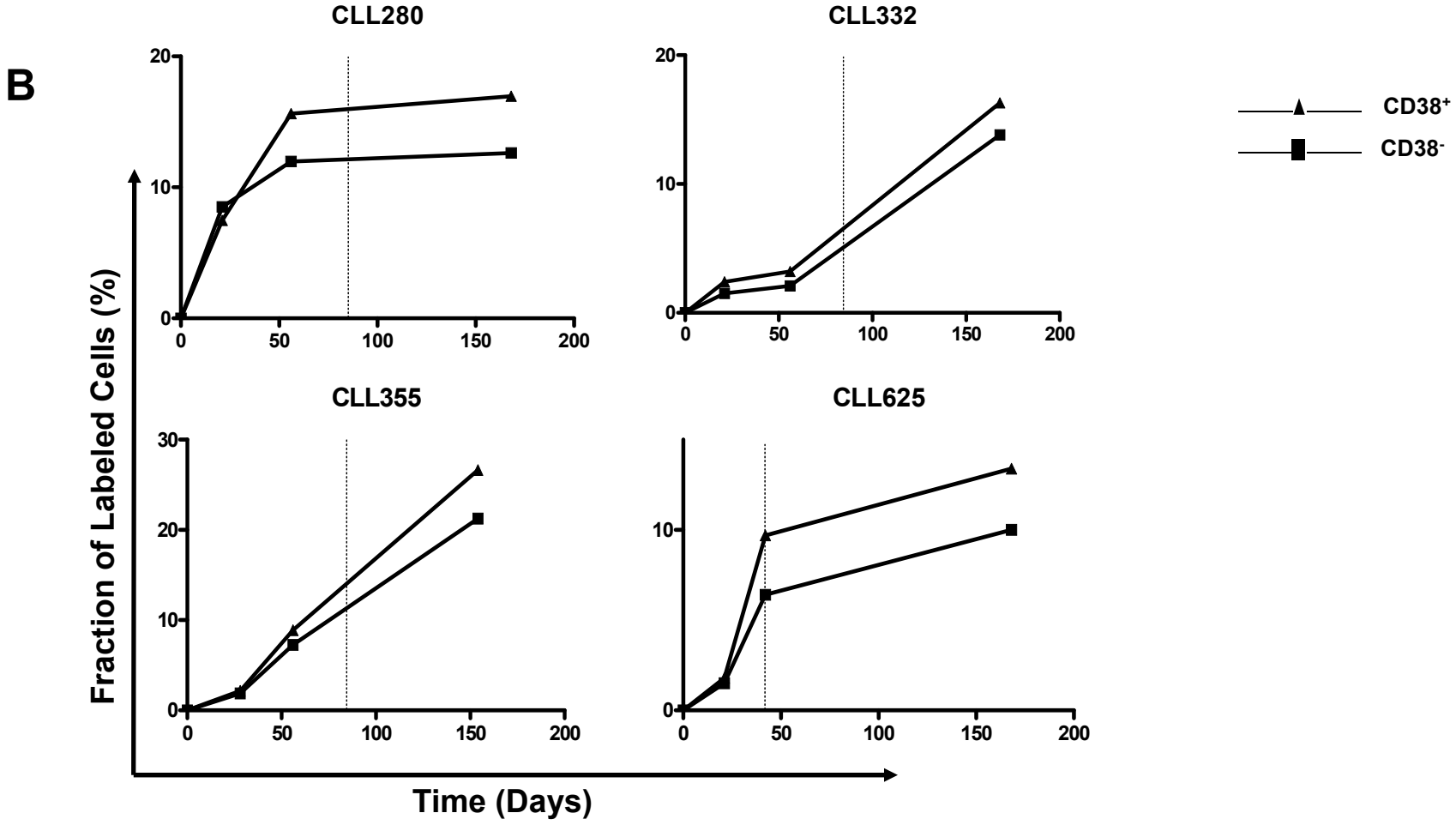

Group B

Calissano *et al.* Fig. 4